research communications

Synthesis, crystal structure and Hirshfeld surface analysis of 2-[(2,4-dimethylbenzyl)sulfanyl]-pyrimidine-4,6-diamine

Gulrukh Salieva,[a,b] Tursunali Kholikov,[a] Rasul Ya Okmanov,[c] Alimjon Matchanov,[d] Khamid U Khodjaniyazov,[d] Shakhnoza Kadirova[a] and Batirbay Torambetov[a]*

[a]National University of Uzbekistan named after Mirzo Ulugbek, 4 University St, Tashkent, 100174, Uzbekistan, [b]Tashkent Medical Academy, 2 Farabi St, Tashkent, 100109, Uzbekistan, [c]S. Yunusov Institute of the Chemistry of Plant Substances, Academy of Sciences of Uzbekistan, Mirzo Ulugbek St 77, Tashkent 100170, Uzbekistan, and [d]Institute of Bioorganic Chemistry, Academy of Sciences of Uzbekistan, M. Ulugbek St, 83, Tashkent, 100125, Uzbekistan. *Correspondence e-mail: torambetov_b@mail.ru

The title compound, $C_{13}H_{16}N_4S$ (DAMP-DMB), was synthesized through the reaction of 2,4-dimethylbenzyl chloride with diaminopyrimidine-thiol. Single-crystal X-ray diffraction analysis confirmed that the compound crystallizes in the monoclinic crystal system, space group $P2_1/c$. The asymmetric unit contains a single molecular entity. Structural examination revealed the presence of a dimeric arrangement consolidated by N—H···N hydrogen-bonding interactions. Additionally, Hirshfeld surface analysis indicated that H···H, N···H, C···H, and S···H contacts account for 98.9% of the total intermolecular interactions to the Hirshfeld surface.

1. Chemical context

Diamino-substituted pyrimidines are pyrimidine derivatives with important applications in pharmaceuticals and organic synthesis (Tolba *et al.*, 2022; Rosowsky *et al.*, 2004). These compounds play a crucial role in medicinal chemistry, in particular because of their antiviral (Hocková *et al.*, 2004), antibacterial (Kandeel *et al.*, 1994), antimalarial (Neekhara *et al.*, 2006) and antimicrobial activities (Holla *et al.*, 2006). Similarly, a 4,6-diaminopyrimidine-based derivative has showed potential antiviral activity against dengue by targeting the NS2B/NS3 protease (Subasri *et al.*, 2017). Some organometallic complexes of diaminopyrimidine-thiol with tin and ruthenium exhibit anticancer activity (Grześkiewicz *et al.*, 2017; Silva *et al.*, 2020). Herein we report the crystal structure and Hirshfeld surface analysis of a newly synthesized organic compound, namely 2-[(2,4-dimethylbenzyl)sulfanyl]pyrimidine-4,6-diamine (DAMP-DMB).
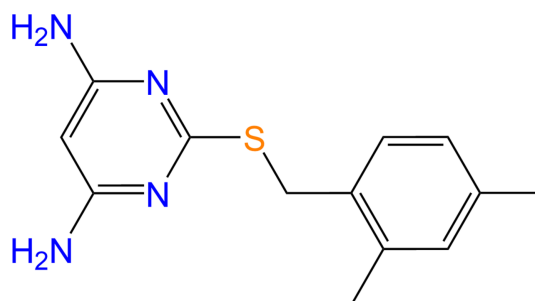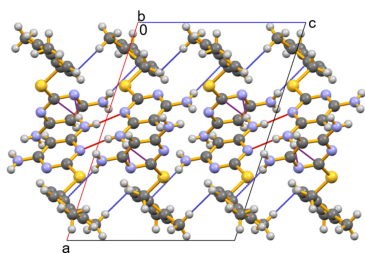
Table 1
Hydrogen-bond geometry (Å, °).

$Cg2$ is the centroid of the C6–C11 ring.

| $D-H\cdots A$	$D-H$	$H\cdots A$	$D\cdots A$	$D-H\cdots A$
C10—H10$\cdots$C1^i	0.93	2.82	3.623 (4)	145
N3—H3$B\cdots$N4^{ii}	0.82 (3)	2.54 (3)	3.340 (5)	168 (3)
N4—H4$A\cdots$N1^{iii}	0.87 (3)	2.56 (3)	3.372 (4)	156 (3)
N4—H4$A\cdots$C4^{iii}	0.87 (3)	2.70 (4)	3.540 (4)	164 (3)
N4—H4$B\cdots$N2^{iv}	0.86 (3)	2.19 (3)	3.039 (3)	172 (3)
N3—H3$A\cdots Cg2^{v}$	0.85 (4)	2.89 (4)	3.561 (3)	137 (3)

Symmetry codes: (i) $x, y+1, z$; (ii) $x, -y-\frac{1}{2}, z-\frac{1}{2}$; (iii) $-x+1, y-\frac{1}{2}, -z+\frac{1}{2}$; (iv) $-x+1, -y, -z+1$; (v) $x, -y+\frac{1}{2}, z-\frac{1}{2}$.

2. Structural commentary

DAMP-DMB (Fig. 1) crystallizes in the monoclinic crystal system, space group $P2_1/c$ (14), with a single molecule in the asymmetric unit. The amine groups on the pyrimidine ring are co-planar and the dihedral angle between the pyrimidine and phenyl rings is 63.03 (14)°. The torsion angles for the groups are N1—C4—S1—C5 = −6.7 (3)° and C11—C6—C5—S1 = −104.2 (3)° respectively. DAMP-DMB contains several hydrogen-bond donor and acceptor groups. However, due to the twisted conformation of the diaminopyrimidine group, the molecule does not exhibit any intramolecular hydrogen-bonding or π-stacking interactions.

3. Supramolecular features

The crystal structure of DAMP-DMB reveals a dimeric association of molecules around the inversion center, where the molecules are connected through moderately strong N4—H4$B\cdots$N2 [H$\cdots A$ = 2.19 (3) Å] hydrogen bonds (Fig. 2a, Table 1) (Steiner, 2002). In the dimeric association of DAMP-DMB molecules, the ring pattern contains a total of eight atoms, two of them are donors, two are acceptors, hence the graph-set notation is R_2^2 (8) (Bernstein et al., 1995). These dimeric units are further stabilized by N—H$\cdots\pi$ interactions, specifically between the amine hydrogen atom of the pyrimidine ring and the π-electron cloud of the benzene ring [N3—H3$A\cdots Cg2$, H$\cdots Cg$ = 2.89 (4) Å]. Similarly, as observed in the 2D finger print plots (see Section 4), the crystal structure also contains hydrogen-bonding interactions
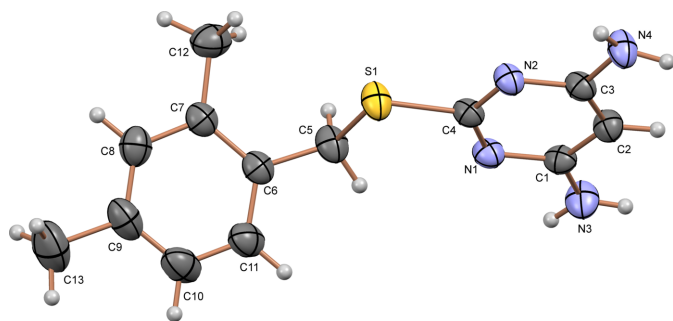
Figure 1
The molecular structure of DAMP-DMB, with atomic displacement ellipsoids drawn at the 30% probability level, showing the atom labeling. Hydrogen atoms are represented as small spheres with arbitrary radii.
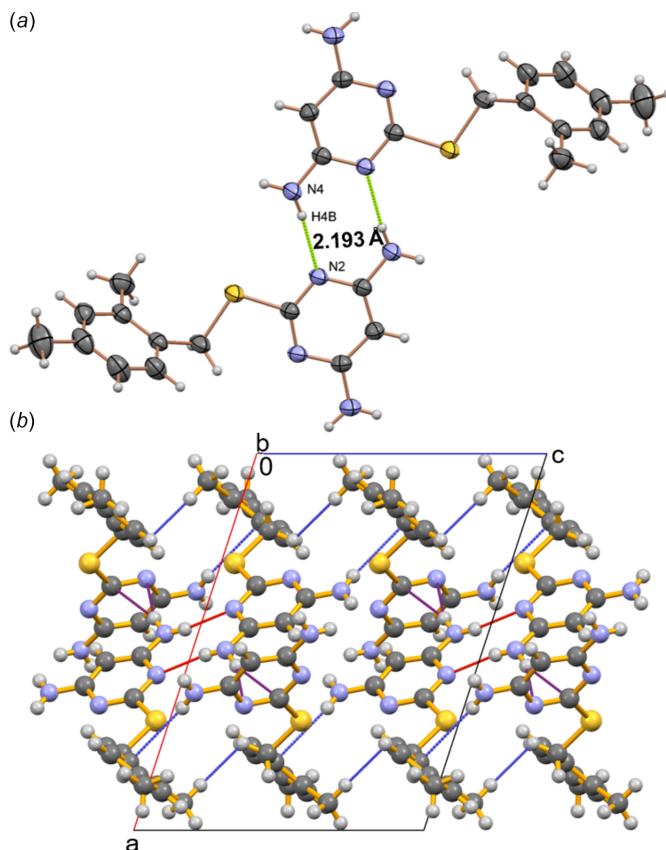
Figure 2
(a) The association between the molecules of DAMP-DMB to form a dimer involving N4—H4$B\cdots$N2 interactions and (b) view of the packing of molecules and association of dimeric units along the c axis in the crystal structure of DAMP-DMB.

specifically, N—H$\cdots$N interactions [N4—H4$A\cdots$N1, H$\cdots A$ = 2.56 (3) Å]. Furthermore, the crystal structure exhibits intermolecular H$\cdots$H interactions involving the methyl hydrogen and and the hydrogen atom of the methylene spacer. (Fig. 2b). This hierarchical organization, governed by multiple weak intermolecular interactions, including H$\cdots$H, N$\cdots$H, C$\cdots$H, and S$\cdots$H, plays a crucial role in the overall packing and cohesion of the crystal structure.

4. Hirshfeld surface analysis

A Hirshfeld surface analysis (Spackman & Jayatilaka, 2009) was performed and fingerprint plots (Spackman & McKinnon, 2002) generated using CrystalExplorer 21.5 (Spackman et al., 2021) to investigate the interactions contributing to the cohesion of the crystal structure. The Hirshfeld surface and fingerprint plots are shown in Figs. 3 and 4. The presence of red spots on the Hirshfeld surface indicates close N$\cdots$H contacts, which are also reflected in the corresponding 2D fingerprint plots. The molecule predominantly engages in H$\cdots$H, C$\cdots$H, N$\cdots$H, and S$\cdots$H interactions, contributing 51.6%, 23.0%, 15.8%, and 8.5%, respectively to the Hirshfeld surface, accounting for 98.9% of the total interactions. In contrast, interactions such as C$\cdots$C and C$\cdots$N collectively
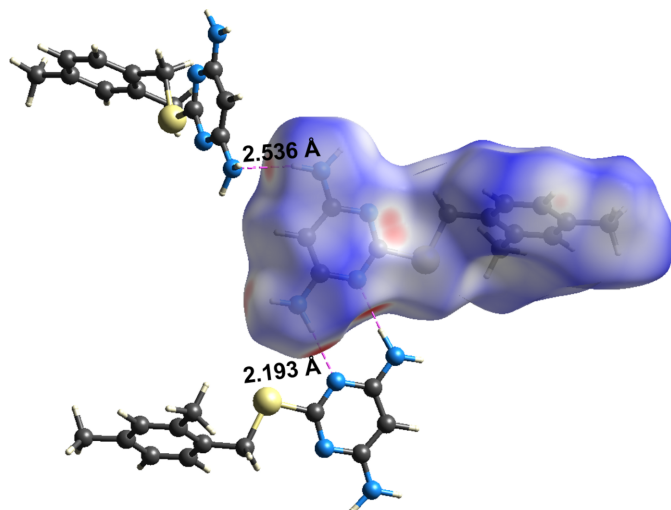
Figure 3
Visualization of the three-dimensional Hirshfeld surfaces for DAMP-DMB.

account for only 0.9%, indicating their minimal role in crystal-structure cohesion. The 2D fingerprint plots reveals the presence of distinct hydrogen-bonding spikes corresponding to N—H···N interactions. The lower right spike at (d_i, d_e) = (1.2, 0.8), represents the hydrogen-bond acceptor, while the upper left spike at (d_i, d_e) = (0.8, 1.8) corresponds to the hydrogen-bond donor. Similarly, a sharp feature along the diagonal in the lower left region indicates a close H···H contact, shorter than 2.4 Å, where $d_i = d_e \simeq 1.2$ Å (Figs. 3 and 4).
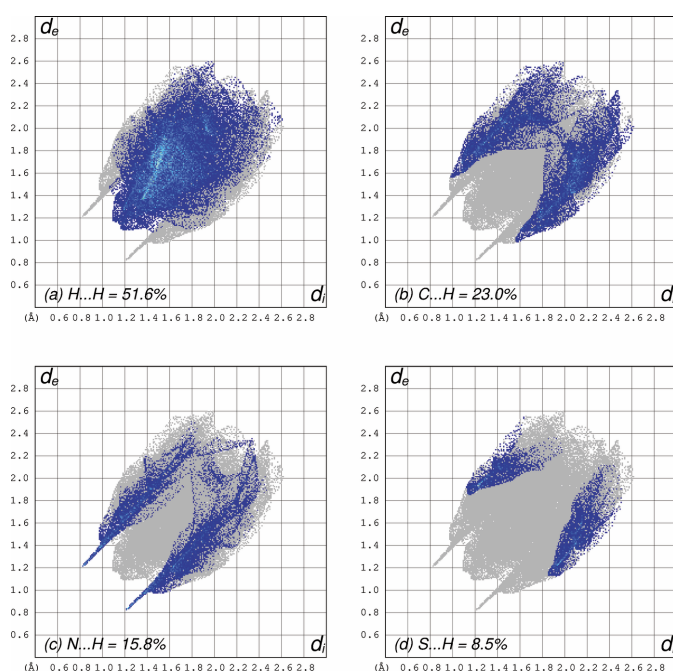

Figure 4
Two-dimensional fingerprint plots of the Hirshfeld surfaces for DAMP-DMB showing the contributions of various hydrogen-bonding interactions.

5. Database survey

A survey of the Cambridge Structural Database (CSD, Version 5.45, last updated March 2024; Groom *et al.*, 2016) using ConQuest (Bruno *et al.*, 2002) revealed 32 crystal structures for the diaminopyrimidine-thiol (DAMP) fragment; among which, eleven structures are related to organometallic compounds. Out of the eleven structures, two complexes of the diaminopyrimidine thiol ligand with triphenyl tin and one with trimethyl tin are reported where the sulfur atom binds monodentately with the metal atom (CEHZIB, Grześkiewicz *et al.*, 2017; VUFTAT, VUFTEX, Ioannidou *et al.*, 2013). Similarly, three structures with ruthenium and two with cobalt metal centers are reported where the metal is coordinated bidentately with N and S atoms (FEGQER, Silva *et al.*, 2020; JACCAV, Ribeiro *et al.*, 2020; XOTDAO, da Silva *et al.*, 2019; TIYJUG01, Yamanari *et al.*, 2002; COHBEK, Gioftsidou *et al.*, 2024). Interestingly, one crystal structure with a Cu metal atom is reported where the diaminopyrimidine thiol derivative binds with the metal atom in a bidentate fashion through the nitrogen atoms (DEDRAI, Moyaert *et al.*, 2017). Two structures of a diaminopyrimidine thiol derivative containing zinc are also deposited (TAGBUY, Romero *et al.*, 1990; ZIKFII, Salas *et al.*, 1995). Similarly, twelve crystal structures of DAMP with amides have been reported. In addition, one crystal structure having two DAMP fragments connected *via* a bridging methylene (–CH$_2$–) group are reported. There are also structures for methyl and ethyl derivatives directly connected to the thiol group of the DAMP fragment. However, no crystal structures of DAMP derivatives with 2,4-dimethylbenzyl have been reported.

6. Synthesis and crystallization

A round-bottomed flask equipped with a magnetic stirrer was charged with diaminopyrimidine-thiol (50.0 mg, 0.351 mmol) dissolved in a mixture of 1.0 *N* aqueous NaOH (0.35 mL, 0.35 mmol) and methanol (5.0 mL). The reaction mixture was stirred at room temperature for 1 h and then concentrated *in vacuo* to afford a tan solid. The resulting solid was dissolved in DMF (5.0 mL), treated with 2,4-dimethylbenzyl chloride (50.0 µL, 0.35 mmol), and stirred at room temperature for 2 h. The reaction progress was monitored by TLC. Upon completion, the DMF was removed *in vacuo*, and the residue was partitioned between water (50 mL) and chloroform (3 × 50 mL). The combined organic extracts were dried over Na$_2$SO$_4$, filtered, and concentrated under vacuum. The residue was further dried at room temperature for 48 h, yielding the product as colorless crystals (90%) (Salieva *et al.*, 2025).

^{1}H-NMR (600 MHz, CD$_3$OD) δ: 2.23 (*s*, 3H, CH$_3$), 2.30 (*s*, 3H, CH$_3$), 4.27 (*s*, 2H, S-CH$_2$) 5.29 (*s*, 1H, CH pyrimidine), 6.88 (*d*, *J* = 6 Hz, 1H, Ar), 6.93 (*s*, 1H, Ar), 7.17 (*d*, *J* = 12 Hz, H, CH Ar) ^{13}C NMR (150 MHz, CD$_3$OD) δ: 18.0, 19.7, 32.4, 79.2, 126.3, 129.7, 130.6, 132.3, 136.4, 136.7, 163.8, 169.6. LC-MC (Q-TOF) *m/z*; [*M+H+*] calculated C$_{13}$H$_{17}$N$_4$S$^+$ = 261.116, found 261.118.

Table 2
Experimental details.

Crystal data
Chemical formula	$C_{13}H_{16}N_4S$
M_r	260.36
Crystal system, space group	Monoclinic, $P2_1/c$
Temperature (K)	293
a, b, c (Å)	14.482 (3), 9.3850 (19), 10.590 (2)
β (°)	108.07 (3)
V (Å³)	1368.3 (5)
Z	4
Radiation type	Cu $K\alpha$
μ (mm⁻¹)	2.00
Crystal size (mm)	$0.2 \times 0.1 \times 0.07$

Data collection
Diffractometer	Bruker D8 VENTURE dual wavelength Mo/Cu
Absorption correction	Multi-scan (*SADABS*; Krause et al., 2015)
T_{min}, T_{max}	0.64, 0.87
No. of measured, independent and observed [$I > 2\sigma(I)$] reflections	37911, 2329, 2057
R_{int}	0.040
$(\sin \theta/\lambda)_{max}$ (Å⁻¹)	0.595

Refinement
$R[F^2 > 2\sigma(F^2)]$, $wR(F^2)$, S	0.049, 0.149, 1.08
No. of reflections	2329
No. of parameters	181
H-atom treatment	H atoms treated by a mixture of independent and constrained refinement
$\Delta\rho_{max}$, $\Delta\rho_{min}$ (e Å⁻³)	0.57, −0.21

Computer programs: *APEX5* and *SAINT* (Bruker, 2016), *SHELXT2018/2* (Sheldrick, 2015a), *SHELXL2018/3* (Sheldrick, 2015b) and *OLEX2* (Dolomanov et al., 2009).

Elemental analysis: calculated; $C_{13}H_{16}N_4S$ = 260.1168, C, 59.97; H, 6.19; N, 21.52; S, 12.31%. Found; $C_{13}H_{16}N_4S$ = 260.1168, C, 59.8882; H, 6.0750; N, 21.3749; S, 12.3001%.

7. Refinement

Crystal data, data collection and structure refinement details are summarized in Table 2. H atoms were refined isotropically by a mixture of independent and constrained refinement.

References

Bernstein, J., Davis, R. E., Shimoni, L. & Chang, N. L. (1995). *Angew. Chem. Int. Ed. Engl.* **34**, 1555–1573.

Bruker (2016). *APEX5* and *SAINT*. Bruker AXS Inc. Madison, Wisconsin, USA.

Bruno, I. J., Cole, J. C., Edgington, P. R., Kessler, M., Macrae, C. F., McCabe, P., Pearson, J. & Taylor, R. (2002). *Acta Cryst.* **B58**, 389–397.

Dolomanov, O. V., Bourhis, L. J., Gildea, R. J., Howard, J. A. K. & Puschmann, H. (2009). *J. Appl. Cryst.* **42**, 339–341.

Gioftsidou, D. K., Kallitsakis, M. G., Kavaratzi, K., Hatzidimitriou, A. G., Terzidis, M. A., Lykakis, I. N. & Angaridis, P. A. (2024). *Dalton Trans.* **53**, 1469–1481.

Groom, C. R., Bruno, I. J., Lightfoot, M. P. & Ward, S. C. (2016). *Acta Cryst.* **B72**, 171–179.

Grześkiewicz, A. M., Owczarzak, A., Kucińska, M., Murias, M. & Kubicki, M. (2017). *J. Coord. Chem.* **70**, 1776–1789.

Hocková, D., Holý, A. N., Masojídková, M., Andrei, G., Snoeck, R., De Clercq, E. & Balzarini, J. (2004). *Bioorg. Med. Chem.* **12**, 3197–3202.

Holla, B. S., Mahalinga, M., Karthikeyan, M. S., Akberali, P. M. & Shetty, N. S. (2006). *Bioorg. Med. Chem.* **14**, 2040–2047.

Ioannidou, A., Czapik, A., Gkizis, P., Perviaz, M., Tzimopoulos, D., Gdaniec, M. & Akrivos, P. D. (2013). *Aust. J. Chem.* **66**, 600–606.

Kandeel, M., El-Meligie, S., Omar, R., Roshdy, S. & Youssef, K. (1994). *J. Pharm. Sci.* **3**, 197–205.

Krause, L., Herbst-Irmer, R., Sheldrick, G. M. & Stalke, D. (2015). *J. Appl. Cryst.* **48**, 3–10.

Moyaert, T. E., Paul, C., Chen, W., Sarjeant, A. A. & Dawe, L. N. (2017). *Acta Cryst.* **E73**, 1534–1538.

Neekhara, R., Mishra, B. J. & Narayana, N. H. (2006). *Asian J. Chem.* **18**(2), 1167–1173.

Ribeiro, G. H., Guedes, A. P., de Oliveira, T. D., de Correia, C. R. B. b, Colina-Vegas, L., Lima, M. A., Nóbrega, J. A., Cominetti, M. R., Rocha, F. V., Ferreira, A. G., Castellano, E. E., Teixeira, F. R. & Batista, A. A. (2020). *Inorg. Chem.* **59**, 15004–15018.

Romero, M. A., Salas, J. M., López, R., Gutiérrez, M. D., Panneerselvam, K., Chacko, K. K., Aoki, K. & Yamazaki, H. (1990). *Inorg. Chim. Acta*, **172**, 253–258.

Rosowsky, A., Forsch, R. A., Sibley, C. H., Inderlied, C. B. & Queener, S. F. (2004). *J. Med. Chem.* **47**, 1475–1486.

Salas, J. M., Romero, M. A. & Faure, R. (1995). *Acta Cryst.* **C51**, 2532–2534.

Salieva, G., Uktamova, M., Torikai, K. & Kholikov, T. (2025). *Molbank*, **2025**, M1965.

Sheldrick, G. M. (2015a). *Acta Cryst.* **A71**, 3–8.

Sheldrick, G. M. (2015b). *Acta Cryst.* **C71**, 3–8.

Silva, M. M. da, de Camargo, M. S., Correa, R. S., Castelli, S., De Grandis, R. A., Takarada, J. E., Varanda, E. A., Castellano, E. E., Deflon, V. M., Cominetti, M. R., Desideri, A. & Batista, A. A. (2019). *Dalton Trans.* **48**, 14885–14897.

Silva, M. M. D., Camargo, M. S. D., Castelli, S., Grandis, R. A. D., Castellano, E. E., Deflon, V. M., Cominetti, M. R., Desiderib, A. & Batista, A. A. (2020). *J. Braz. Chem. Soc.* **31**, 536–549.

Spackman, M. A. & Jayatilaka, D. (2009). *CrystEngComm*, **11**, 19–32.

Spackman, M. A. & McKinnon, J. J. (2002). *CrystEngComm*, **4**, 378–392.

Spackman, P. R., Turner, M. J., McKinnon, J. J., Wolff, S. K., Grimwood, D. J., Jayatilaka, D. & Spackman, M. A. (2021). *J. Appl. Cryst.* **54**, 1006–1011.

Steiner, T. (2002). *Angew. Chem. Int. Ed.* **41**, 48–76.

Subasri, S., Kumar, T. A., Sinha, B. N., Jayaprakash, V., Viswanathan, V. & Velmurugan, D. (2017). *Acta Cryst.* **E73**, 306–309.

Tolba, M. S., El-Dean, A., Ahmed, M., Hassanien, R., Sayed, M., Zaki, R., Mohamed, S., Zawam, S. & Abdel-Raheem, S. (2022). *Curr. Chem. Lett.* **11**, 121–138.

Yamanari, K., Kida, M., Fuyuhiro, A., Kita, M. & Kaizaki, S. (2002). *Inorg. Chim. Acta*, **332**, 115–122.

supporting information

Synthesis, crystal structure and Hirshfeld surface analysis of 2-[(2,4-dimethyl-benzyl)sulfanyl]pyrimidine-4,6-diamine

Gulrukh Salieva, Tursunali Kholikov, Rasul Ya Okmanov, Alimjon Matchanov, Khamid U Khodjaniyazov, Shakhnoza Kadirova and Batirbay Torambetov

Computing details

2-[(2,4-Dimethylbenzyl)sulfanyl]pyrimidine-4,6-diamine

Crystal data

$C_{13}H_{16}N_4S$	$F(000) = 552$
$M_r = 260.36$	$D_x = 1.264$ Mg m^{-3}
Monoclinic, $P2_1/c$	Cu $K\alpha$ radiation, $\lambda = 1.54178$ Å
$a = 14.482$ (3) Å	Cell parameters from 9926 reflections
$b = 9.3850$ (19) Å	$\theta = 5.7$–$66.3°$
$c = 10.590$ (2) Å	$\mu = 2.00$ mm^{-1}
$\beta = 108.07$ (3)°	$T = 293$ K
$V = 1368.3$ (5) Å^3	Prism, colourless
$Z = 4$	$0.2 \times 0.1 \times 0.07$ mm

Data collection

Bruker D8 VENTURE dual wavelength Mo/Cu diffractometer	$T_{min} = 0.64$, $T_{max} = 0.87$
	37911 measured reflections
Radiation source: microfocus sealed X-ray tube, INCOATEC IμS	2329 independent reflections
	2057 reflections with $I > 2\sigma(I)$
Graphite monochromator	$R_{int} = 0.040$
Detector resolution: 7.3910 pixels mm^{-1}	$\theta_{max} = 66.6°$, $\theta_{min} = 5.7°$
φ and ω scans	$h = -16 \rightarrow 16$
Absorption correction: multi-scan (SADABS; Krause et al., 2015)	$k = -11 \rightarrow 11$
	$l = -12 \rightarrow 12$

Refinement

Refinement on F^2	Secondary atom site location: difference Fourier map
Least-squares matrix: full	
$R[F^2 > 2\sigma(F^2)] = 0.049$	Hydrogen site location: mixed
$wR(F^2) = 0.149$	H atoms treated by a mixture of independent and constrained refinement
$S = 1.08$	
2329 reflections	$w = 1/[\sigma^2(F_o^2) + (0.068P)^2 + 0.8542P]$ where $P = (F_o^2 + 2F_c^2)/3$
181 parameters	
0 restraints	$(\Delta/\sigma)_{max} < 0.001$
	$\Delta\rho_{max} = 0.57$ e Å^{-3}
	$\Delta\rho_{min} = -0.21$ e Å^{-3}

Special details

Geometry. All esds (except the esd in the dihedral angle between two l.s. planes) are estimated using the full covariance matrix. The cell esds are taken into account individually in the estimation of esds in distances, angles and torsion angles; correlations between esds in cell parameters are only used when they are defined by crystal symmetry. An approximate (isotropic) treatment of cell esds is used for estimating esds involving l.s. planes.

Fractional atomic coordinates and isotropic or equivalent isotropic displacement parameters (Å²)

	x	*y*	*z*	$U_{iso}*/U_{eq}$
S1	0.70925 (6)	0.22323 (8)	0.45344 (7)	0.0692 (3)
N2	0.58768 (15)	0.0155 (2)	0.4032 (2)	0.0564 (5)
N1	0.66759 (16)	0.0540 (2)	0.2395 (2)	0.0577 (5)
N3	0.6348 (2)	−0.0867 (4)	0.0539 (3)	0.0772 (8)
N4	0.4784 (2)	−0.1665 (3)	0.3859 (3)	0.0711 (7)
C4	0.64938 (18)	0.0803 (3)	0.3523 (2)	0.0531 (6)
C1	0.61661 (19)	−0.0562 (3)	0.1686 (2)	0.0562 (6)
C2	0.5520 (2)	−0.1347 (3)	0.2127 (3)	0.0598 (7)
H2	0.518848	−0.211765	0.164224	0.072*
C3	0.53829 (19)	−0.0950 (3)	0.3309 (2)	0.0555 (6)
C6	0.81963 (19)	0.4397 (3)	0.4079 (3)	0.0598 (7)
C7	0.88069 (19)	0.4817 (3)	0.5314 (3)	0.0623 (7)
C8	0.8975 (2)	0.6268 (4)	0.5536 (3)	0.0770 (8)
H8	0.937665	0.657394	0.635863	0.092*
C9	0.8560 (3)	0.7274 (3)	0.4561 (4)	0.0847 (10)
C10	0.7976 (2)	0.6828 (4)	0.3357 (4)	0.0923 (11)
H10	0.770351	0.749011	0.269275	0.111*
C11	0.7789 (2)	0.5421 (4)	0.3123 (4)	0.0805 (9)
H11	0.737651	0.513470	0.230042	0.097*
C5	0.7966 (2)	0.2853 (3)	0.3734 (3)	0.0692 (8)
H5A	0.855552	0.228946	0.403493	0.083*
H5B	0.769744	0.274625	0.277885	0.083*
C12	0.9274 (3)	0.3764 (4)	0.6386 (3)	0.0899 (10)
H12A	0.980309	0.421258	0.704739	0.135*
H12B	0.951482	0.297020	0.600929	0.135*
H12C	0.880392	0.343347	0.678883	0.135*
C13	0.8798 (4)	0.8847 (4)	0.4839 (6)	0.1331 (18)
H13A	0.849016	0.939278	0.405419	0.200*
H13B	0.948811	0.898122	0.508998	0.200*
H13C	0.856385	0.915894	0.554811	0.200*
H3A	0.675 (3)	−0.036 (4)	0.030 (3)	0.085 (11)*
H3B	0.603 (2)	−0.150 (4)	0.007 (3)	0.070 (10)*
H4A	0.437 (2)	−0.222 (3)	0.332 (3)	0.071 (9)*
H4B	0.466 (2)	−0.124 (3)	0.450 (3)	0.072 (9)*

Atomic displacement parameters (Å²)

	U^{11}	U^{22}	U^{33}	U^{12}	U^{13}	U^{23}
S1	0.0831 (5)	0.0680 (5)	0.0734 (5)	−0.0215 (3)	0.0488 (4)	−0.0164 (3)

N2	0.0670 (13)	0.0534 (12)	0.0586 (12)	−0.0058 (10)	0.0338 (10)	−0.0031 (10)
N1	0.0677 (13)	0.0592 (12)	0.0537 (12)	−0.0022 (10)	0.0296 (10)	0.0014 (10)
N3	0.096 (2)	0.0867 (19)	0.0632 (15)	−0.0224 (16)	0.0454 (15)	−0.0157 (14)
N4	0.0889 (18)	0.0677 (15)	0.0719 (16)	−0.0251 (14)	0.0468 (14)	−0.0155 (13)
C4	0.0594 (14)	0.0509 (13)	0.0554 (14)	0.0026 (11)	0.0274 (11)	0.0025 (11)
C1	0.0633 (15)	0.0597 (15)	0.0500 (13)	0.0048 (12)	0.0240 (11)	0.0012 (11)
C2	0.0680 (16)	0.0579 (15)	0.0597 (15)	−0.0052 (12)	0.0288 (12)	−0.0069 (12)
C3	0.0626 (15)	0.0524 (14)	0.0581 (14)	0.0009 (11)	0.0286 (12)	0.0027 (11)
C6	0.0559 (15)	0.0639 (16)	0.0697 (17)	−0.0036 (12)	0.0345 (13)	0.0030 (13)
C7	0.0552 (15)	0.0678 (17)	0.0722 (17)	−0.0032 (12)	0.0317 (13)	0.0024 (13)
C8	0.0640 (18)	0.083 (2)	0.089 (2)	−0.0123 (15)	0.0304 (15)	−0.0116 (17)
C9	0.077 (2)	0.0590 (18)	0.129 (3)	0.0018 (15)	0.047 (2)	0.0057 (19)
C10	0.067 (2)	0.086 (2)	0.119 (3)	0.0026 (17)	0.023 (2)	0.031 (2)
C11	0.0671 (18)	0.085 (2)	0.089 (2)	−0.0080 (16)	0.0251 (16)	0.0186 (18)
C5	0.0748 (18)	0.0703 (18)	0.0786 (19)	−0.0111 (14)	0.0473 (15)	−0.0064 (14)
C12	0.080 (2)	0.111 (3)	0.078 (2)	−0.0021 (19)	0.0240 (17)	0.020 (2)
C13	0.129 (4)	0.072 (2)	0.197 (5)	−0.006 (2)	0.048 (4)	−0.008 (3)

Geometric parameters (Å, º)

S1—C4	1.767 (3)	C7—C8	1.390 (4)
S1—C5	1.823 (3)	C7—C12	1.500 (4)
N2—C4	1.326 (3)	C8—H8	0.9300
N2—C3	1.354 (3)	C8—C9	1.390 (5)
N1—C4	1.323 (3)	C9—C10	1.359 (5)
N1—C1	1.354 (3)	C9—C13	1.524 (5)
N3—C1	1.351 (3)	C10—H10	0.9300
N3—H3A	0.85 (4)	C10—C11	1.355 (5)
N3—H3B	0.82 (3)	C11—H11	0.9300
N4—C3	1.362 (3)	C5—H5A	0.9700
N4—H4A	0.87 (3)	C5—H5B	0.9700
N4—H4B	0.86 (3)	C12—H12A	0.9600
C1—C2	1.381 (4)	C12—H12B	0.9600
C2—H2	0.9300	C12—H12C	0.9600
C2—C3	1.379 (4)	C13—H13A	0.9600
C6—C7	1.390 (4)	C13—H13B	0.9600
C6—C11	1.388 (4)	C13—H13C	0.9600
C6—C5	1.505 (4)		
C4—S1—C5	103.99 (13)	C9—C8—H8	119.1
C4—N2—C3	115.2 (2)	C8—C9—C13	119.7 (4)
C4—N1—C1	114.6 (2)	C10—C9—C8	119.2 (3)
C1—N3—H3A	119 (2)	C10—C9—C13	121.1 (4)
C1—N3—H3B	118 (2)	C9—C10—H10	119.9
H3A—N3—H3B	122 (3)	C11—C10—C9	120.2 (3)
C3—N4—H4A	115 (2)	C11—C10—H10	119.9
C3—N4—H4B	115 (2)	C6—C11—H11	119.1
H4A—N4—H4B	122 (3)	C10—C11—C6	121.7 (3)

N2—C4—S1	111.56 (18)	C10—C11—H11	119.1
N1—C4—S1	119.41 (19)	S1—C5—H5A	109.8
N1—C4—N2	129.0 (2)	S1—C5—H5B	109.8
N1—C1—C2	122.0 (2)	C6—C5—S1	109.16 (19)
N3—C1—N1	115.8 (3)	C6—C5—H5A	109.8
N3—C1—C2	122.1 (3)	C6—C5—H5B	109.8
C1—C2—H2	121.1	H5A—C5—H5B	108.3
C3—C2—C1	117.8 (2)	C7—C12—H12A	109.5
C3—C2—H2	121.1	C7—C12—H12B	109.5
N2—C3—N4	115.5 (2)	C7—C12—H12C	109.5
N2—C3—C2	121.4 (2)	H12A—C12—H12B	109.5
N4—C3—C2	123.0 (3)	H12A—C12—H12C	109.5
C7—C6—C5	122.0 (3)	H12B—C12—H12C	109.5
C11—C6—C7	119.5 (3)	C9—C13—H13A	109.5
C11—C6—C5	118.5 (3)	C9—C13—H13B	109.5
C6—C7—C8	117.7 (3)	C9—C13—H13C	109.5
C6—C7—C12	122.1 (3)	H13A—C13—H13B	109.5
C8—C7—C12	120.2 (3)	H13A—C13—H13C	109.5
C7—C8—H8	119.1	H13B—C13—H13C	109.5
C7—C8—C9	121.8 (3)		
N1—C1—C2—C3	1.8 (4)	C7—C6—C5—S1	76.3 (3)
N3—C1—C2—C3	−179.9 (3)	C7—C8—C9—C10	−0.2 (5)
C4—S1—C5—C6	154.6 (2)	C7—C8—C9—C13	−177.8 (3)
C4—N2—C3—N4	176.9 (2)	C8—C9—C10—C11	1.1 (5)
C4—N2—C3—C2	−0.4 (4)	C9—C10—C11—C6	−1.3 (5)
C4—N1—C1—N3	−179.1 (3)	C11—C6—C7—C8	0.4 (4)
C4—N1—C1—C2	−0.8 (4)	C11—C6—C7—C12	−179.7 (3)
C1—N1—C4—S1	−178.90 (18)	C11—C6—C5—S1	−104.2 (3)
C1—N1—C4—N2	−1.1 (4)	C5—S1—C4—N2	175.2 (2)
C1—C2—C3—N2	−1.2 (4)	C5—S1—C4—N1	−6.7 (3)
C1—C2—C3—N4	−178.3 (3)	C5—C6—C7—C8	179.9 (2)
C3—N2—C4—S1	179.62 (18)	C5—C6—C7—C12	−0.2 (4)
C3—N2—C4—N1	1.7 (4)	C5—C6—C11—C10	−179.0 (3)
C6—C7—C8—C9	−0.6 (4)	C12—C7—C8—C9	179.5 (3)
C7—C6—C11—C10	0.5 (5)	C13—C9—C10—C11	178.8 (4)

Hydrogen-bond geometry (Å, º)

*Cg*2 is the centroid of the C6–C11 ring.

D—H⋯A	D—H	H⋯A	D⋯A	D—H⋯A
C10—H10⋯C1i	0.93	2.82	3.623 (4)	145
N3—H3B⋯N4ii	0.82 (3)	2.54 (3)	3.340 (5)	168 (3)
N4—H4A⋯N1iii	0.87 (3)	2.56 (3)	3.372 (4)	156 (3)
N4—H4A⋯C4iii	0.87 (3)	2.70 (4)	3.540 (4)	164 (3)

N4—H4*B*···N2ⁱᵛ	0.86 (3)	2.19 (3)	3.039 (3)	172 (3)
N3—H3*A*···*Cg*2ᵛ	0.85 (4)	2.89 (4)	3.561 (3)	137 (3)

Symmetry codes: (i) x, $y+1$, z; (ii) x, $-y-1/2$, $z-1/2$; (iii) $-x+1$, $y-1/2$, $-z+1/2$; (iv) $-x+1$, $-y$, $-z+1$; (v) x, $-y+1/2$, $z-1/2$.